

# CISS MR

;

1

2

CISS MR

6, 1.5 Tesla MR  
T1 T2 CISS (TR/TE/FA:12.3 msec/5.9 msec/70°)

(conspicuity)

(contrast)

(visibility)

4

1

1

CISS

가

T1

T2, CISS 0.12, 0.06, 0.52, CISS  
(P < 0.05).

CISS

CISS

가

(epidermoid tumor)

T1- T2-

CISS(constructive interference

in steady state:

CISS)

T2

1mm

(Diffusion Weighted

Image)

CISS MR

(motion arti-  
(1,2).

fact)

1996 9 1997 8  
(cerebellopontine angle)

6  
(prepontine cistern)

1998 8 4 1998 12 11

2:4

CISS MR

19 58 43.8 . 6 SI\* : signal intensity (CSF)

가 (Table 1). (round region of interest) (25-35 mm) 4

1.5Tesla MR (Magne- tom vision, Siemens, Erlangen, Germany)

T1 T2 CISS 4 (arachnoid cyst) ±

. CISS (repetition time: TR) 12.3msec, (echo time : TE) 5.9 msec, Duncan Kruskal-Wallis 1-Way test 95% (p<0.05)

(slice thickness) 1.0 mm, (flip angle) 70 ,

(acquisition time, TA) 5 23 T1

TR 513msec, TE 12msec, 5.0 mm,

TA 3 32 T2 TR

4000msec, TE 99msec, 5.0 mm, TA 2 50 . CISS MR

(NEX) 2 matrix CISS 4 , 1

(190x256) CISS (205x256), (FOV) , 1

(175x200) CISS (160x160) . (Table 1)

MR 가 CISS MR , 2 , 2 , 1

(signal intensity), (contour), , 1 , 2

(cranial nerve) (vasculature) . , , , (in-

MR vagination) 3 (Fig. 1).

(conspicuity) 3 ( , , )

가 가 ;

가

grade I (poor: ), (grade I) (grade II)

가

가 grade III (excellent: )

grade II (fair: )

(CSF) (con- 가 6 (grade III) 가

trast) 3 . , , , ,

(Table 2 & Fig. 2).

Table 1. Clinical Findings & Locations of Intracranial Epidermoid Tumor.

Pt	Age	Sex	Symptoms	Location of tumor
1	53	F	Rt. trigeminal neuralgia(V3)	Rt. C-P angle
2	34	F	Rt. trigeminal neuralgia(V2,,V3,)	Prepontine cistern Both C-P angle
3	45	F	Rt. facial palsy	Lt. C-P angle
4	54	M	Lt. trigeminal neuralgia(V3)	Lt. C-P angle
5	58	F	Hearing disturbance (Both)Lt. diplopia	Lt. Prepontine cistern
6	19	M	Hearing disturbance (Lt.)	Lt. C-P angle

\*C-P angle indicates cerebellopontine angle

= [SI\* of CSF-SI of tumor]/SI of CSF

CISS 0.41-0.55  
 $0.52 \pm 0.52$ , T1/T2 0.03-  
 $0.33(0.12 \pm 0.12)$  0.03-0.15( $0.06 \pm 0.05$ )  
 CISS T1 T2  
 (p < 0.05,  
 Table 3).  
 (suprasellar  
 lar cistern), (parasellar region)  
 가  
 (ambient cistern)

Table 2. The Results of Qualitative Analysis.

	Spin- Echo image		CISS image
	T1WI	T2WI	
I	4	5	0
II	2	1	0
III	0	0	6

\*I (poor); tumor not seen or only suspected by widening of subarachnoid space

\*II (fair); tumor vaguely seen but, not its exact extent in the subarachnoid space

\*III (excellent); tumor demarcated with clear margin

CT CSF  
 (delineation)가 (3).  
 (4). 1987 가  
 MR CT (5,6).  
 MR  
 가  
 T1, T2 가  
 가  
 (1).  
 T1 T2 가  
 2DFT MR  
 가 가 CT 2DFT

Table 3. Comparison of Sequence Performance for the Contrast of Epidermoid Tumor to CSF

Pulse Sequence	Contrast (Sd/SCSF)
T1-weighted SE	0.03-0.33 (mean ; $0.12 \pm 0.12$ )
T2-weighted SE	0.03-0.15 (mean ; $0.06 \pm 0.05$ )
CISS image	0.41-0.55 (mean ; $0.52 \pm 0.52$ )

\*Contrast(Sd/SCSF) ; Epidermoid to CSF signal difference to CSF signal ratios

\*SE ; spin-echo image

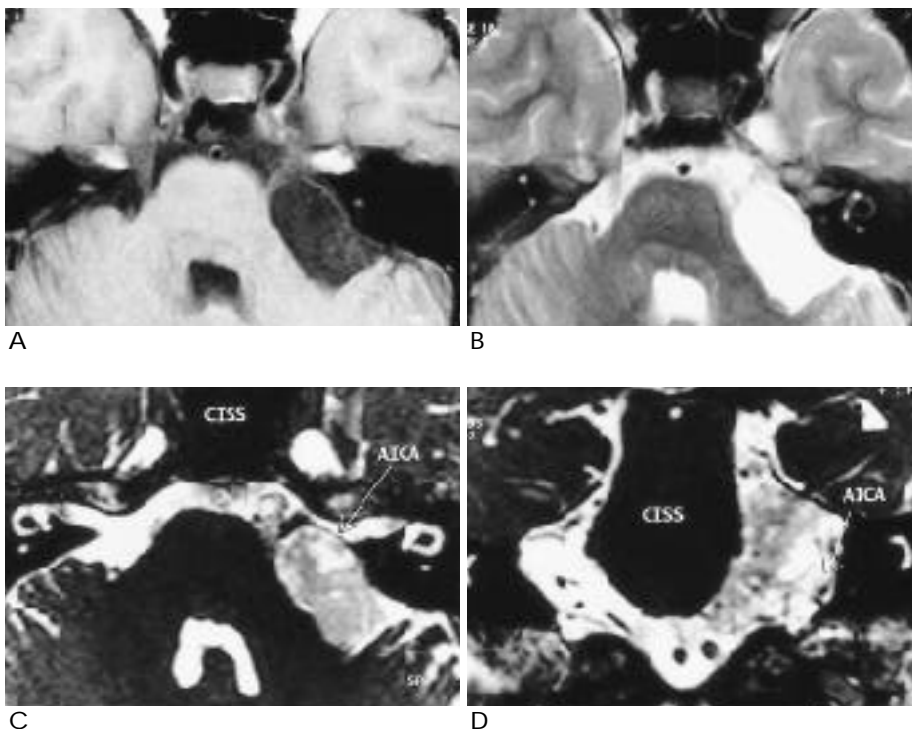


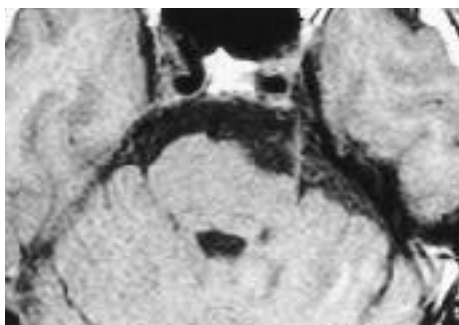
Fig. 1. Case 3 : Epidermoid in the left cerebellopontine angle cistern The spin-echo T1WI(A) and T2WI(B) show the tumor in the left cerebellopontine cistern, which is isointense with CSF. Tumor was suspected because of widening of the subarachnoid space. On CISS axial(C) and coronal(D) images, the tumor is hypointense compared with CSF and hyperintense compared with brain parenchyma. Tumor's extension and relation with adjacent vessel (AICA; arrow) are well seen.

CISS MR

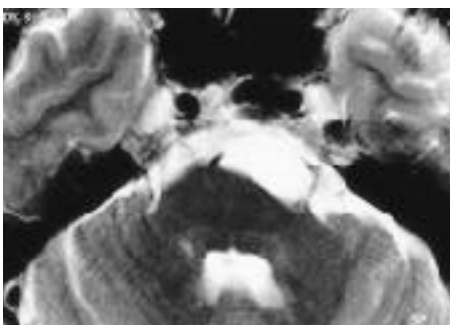
90° RF pulse, rephaser (phase encoding gradient), phase encoding, dephasing

(7,8). T2 ing 가 (9,10). T2 TR (flip angle) FISP FLASH proton density 가 T2 (signal contrast) T2 가 T2 가 T1 가 (16). True FISP FISP PSIF (reversed FISP) FISP가 (15,17).

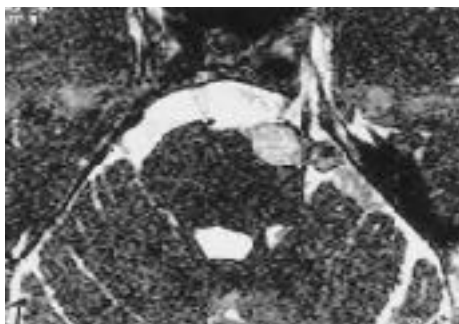
echo train, 3 mm 가, (11,12). FLAIR inversion-recovery sequence T2 FLAIR Ikushima (13) CNR, (local field inhomogeneity) TR, (18). CISS TR, dephasing true FISP PSIF echoes가 (dark line banding artifact) 가 alternating RF pulse nonalternating RF true FISP



A



B



C



D

Fig. 2. Case 5 : Epidermoid in the left prepontine cistern On the conventional spin-echo T1WI(A) and T2WI(B), the tumor in the left prepontine cistern is isointense with CSF. On CISS axial(C) and coronal(D) images, the tumor is hypointense compared with CSF and hyperintense compared with brain parenchyma. The CISS coronal image clearly shows the relation with adjacent vessel (AICA; arrow) and cranial nerve(CN V;arrow).

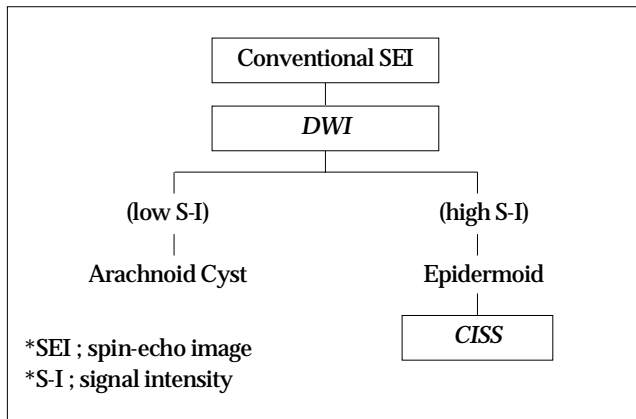


Fig. 3. Flow chart for diagnosis of Epidermoid tumor(C-P angle mass)

keratin , susceptibility 가  
cholesterol crystals keratin  
(13). CISS ( :0.52) 가  
T1 T2 0.12  
0.06 . CISS  
가 , Jung (21) CISS  
(voluminous) 가  
T2  
T2  
3 mm  
CISS 가  
가  
CISS ,  
CISS 가  
(Fig. 3).

(11). FISP image 가  
가 gradient echo image가  
T2 T2 가  
(17). CISS 0.5mm  
가 (11, 19). CISS  
가  
(11, 20). CISS  
가 , grade I( ) II( )  
, CISS  
grade III( )  
( , , ) ( )  
(Table 1).  
CISS  
, CISS  
T2 echo time 99  
milliseconds T2 value  
CISS T2  
가 가  
가 cholesterol crystals

- David F. Kallmes, James M. Provenzale, Harry J. Cloft, Roger E. McClendon. Typical and Atypical MR Imaging Features of Intracranial Epidermoid Tumors. *AJR* 1997;169:883-887
- Jay S. Tsuruda, Wil M. Chew, Michael E. Moseley, David Norman. Diffusion-Weighted MR imaging of the Brain: Value of differentiating between Extraaxial cysts and Epidermoid. *AJNR* 1990;11:925-931 tumors
- Berger MS, Wilson CB. Epidermoid cysts of the posterior fossa. *Neurosurgery* 1985;62:214-219
- Gao P-Y, Osborn A G, Smimitopoulos JG, Harris CP, Radiologic-Pathologic Correlation: epidermoid tumor of the Cerebellopontine Angle. *AJNR* 1992;13:863-872
- Steffey DJ, De Flipp GJ, Sepera T, Gabrielsen TO. MR imaging of primary epidermoid tumors. *J Comput Assist Tomogr* 1988; 12(3):438-440
- Tampieri D, Melanson D, Ethier R, MR imaging of epidermoid cysts. *AJNR* 1989;10:282-285
- Tanioka, Shrakawa T, Machida Y. Three dimensional reconstructed MR imaging of the inner ear. *Radiology* 1991;178:141-144
- Brogan M, Chakeres DW, Schmalbrock P. High-resolution 3DFT MR imaging of the endolymphatic duct and the soft tissue of the optic capsule. *AJNR* 1991;12:1-11
- Mukherji SK, Tart RP, Fitzsimmons J, Beldon C, McGorray S, Guy J, Mancuso AA. Fat-suppressed MR of the orbit and cavernous sinus: comparison of fast spin-echo and conventional spin-echo. *AJNR* 1995;15:1707-1714
- Ross MR, Schomer DF, Chappell P, Enzmann DR. MR imaging of head and neck tumors: comparison of T1-weighted contrast-enhanced fat-suppressed images with conventional T2-weighted and fast spin-echo T2-weighted images. *AJR* 1994;163:173-178
- Casselman JW, Kruhweide R, Diemling M, Ampe W, Dehanes I, Meeus L. Constructive interference in steady state-3DFT MR imaging of the inner ears and cerebellopontine angle. *AJNR*

- 1993;14:47-57
12. . . . .  
Constructive Interference in Steady State (CISS)-3DFT  
1997;37:423-428
13. Ikushima I, Korogi Y, Hirai T, Sugahara T, Shigematsu Y, Komohara Y. MR of Epidermoids with a variety of Pulse Sequences. *AJNR* 1997;18:1359-1363
14. Gyndel ML. The application of steady-state free precession in rapid 2DFT NMR imaging:FAST and SSFP images. *Magn Reson Imaging* 1988;6:415-419
15. Nakamura H, Murakami T, Ishida T, et al. 3DFT-FISP MRI with gadopentetate dimeglumine in differential diagnosis of small liver tumors. *J Comput Assist Tomogr* 1994;18:49-54
16. Ronald R. Price. Contrast mechanisms in gradient-echo imaging and introduction to fast imaging. *RadioGraphics* 1995;15:165-178
17. Robert R. Edelman, John R. Hesselink, Michael B. Zlatkin. *Clinical Magnetic Resonance Imaging*. 2nd ed. Philadelphia:Saunders 1996:302-324
18. Eckstein F, Sittek H, Milz S, Putz R, Reiser M. The morphology of articular cartilage assessed by magnetic resonance imaging. Reproducibility and anatomical correlation. *Surg Radiol Anat* 1994;16:429-438
19. Oppelt A, Groumann R, Varfuss H, Fisher H, Hartl W, Schajor W. FISP, a new fast MRI image. *Electromedica* 1986;54:15-18
20. Casselman JW, Kuhweide R, Dehaene I, Ampe W, Devlies F. Magnetic resonance examinaion of the inner ear and cerebellopontine angle in patients with vertigo and/or abnormal findings at vestibular testing. *Acta Otolaryngol Suppl* 1994;513:15-27
21. . . . .  
MR CISS  
1998;38:595-600

## **CISS MR Imaging Findings of Epidermoid Tumor : Comparison with Spin-Echo Images<sup>1</sup>**

Yong Woo Kim, M.D., Hak Jin Kim, M.D., Sang Yoel Choi, M.D., Jin Sam Heo, M.D.  
Hoon Sik Jung, M.D., Jong Wha Lee, M.D.<sup>2</sup>, Suck Hong Lee, M.D., Byung Soo Kim, M.D.

<sup>1</sup>Department of Diagnostic Radiology, College of Medicine, Pusan National University

<sup>2</sup>Department of Diagnostic Radiology, Ulsan University Hospital

**Purpose :** To evaluate CISS MR imaging findings of epidermoid tumor in comparison with conventional spin-echo images.

**Materials and Methods :** We studied 6 cases of epidermoid tumor in the subarachnoid space. We used a 1.5 T MR unit to obtain CISS images(TR/TE/FA ; 12.3msec/5.9 msec/700) and T1- and T2-weighted spin-echo images. CISS MR imaging findings were evaluated with respect to tumor's signal intensity, contour, and relation with adjacent structures. Conspicuity of the tumor was compared between CISS and spin-echo images. A quantitative analysis was performed by measuring tumor to CSF contrast. In qualitative analysis, three radiologists independently compared CISS image and conventional spin-echo images for visibility of the tumor and graded them into three categories( poor, good, and excellent).

**Results :** Epidermoid tumors were located in the cerebellopontine angle in 4 cases, the prepontine cistern in 1 case, and the cerebellopontine angle-prepontine cistern in 1 case. The tumors were hyperintense relative to brain parenchyma and hypointense relative to CSF on CISS images, were lobulated, encased adjacent cranial nerve and vessels, and invaginated into brain parenchyma. In qualitative analysis, CISS images showed clear demarcation between tumor and CSF, exact tumor extension, and tumor's relation with cranial nerves and vessels better than conventional spin-echo images. In quantitative analysis, the mean contrast values of tumor to CSF on T1-, T2-weighted images, and CISS images were 0.12, 0.06, and 0.52, respectively. The contrast value for CISS images was significantly higher than that for T1- and T2-weighted images( $P < 0.05$ ).

**Conclusions :** Epidermoid tumors in the subarachnoid space are better demonstrated on CISS images than on conventional spin-echo images. This special MR sequence can be added as a routine protocol in the diagnosis of subarachnoid epidermoid tumor.

**Index words :** Brain, MR

Magnetic resonance(MR), technology

Magnetic resonance(MR), Three-dimensional

Address reprint requests to : Hak Jin Kim, M.D., Department of Diagnostic Radiology, Pusan National University Hospital  
#1-10, Ami-dong, Seo-ku, Pusan 602-739 Korea.  
Tel. 82-51-240-7371 Fax. 82-51-244-7534 E-mail hakjink@soback.Kornet.nm.kr